

A predictive method for crude oil volatile organic compounds emission from soil: evaporation and diffusion behavior investigation of binary gas mixtures

Haijing Wang · Thomas Fischer · Wolfgang Wieprecht · Detlev Möller

Received: 15 July 2014 / Accepted: 23 December 2014 / Published online: 10 January 2015
© Springer-Verlag Berlin Heidelberg 2015

Abstract Due to their mobility and toxicity, crude oil volatile organic compounds (VOCs) are representative components for oil pipeline contaminated sites detection. Therefore, contaminated location risk assessment, with airborne light detection and ranging (LIDAR) survey, in particular, requires ground-based determinative methods for oil VOCs, the interaction between oil VOCs and soil, and information on how they diffuse from underground into atmosphere. First, we developed a method for determination of crude oil VOC binary mixtures (take *n*-pentane and *n*-hexane as examples), taking synergistic effects of VOC mixtures on polydimethylsiloxane (PDMS) solid-phase microextraction (SPME) fibers into consideration. Using this method, we further aim to extract VOCs from small volumes, for example, from soil pores, using a custom-made sampling device for nondestructive SPME fiber intrusion, and to study VOC transport through heterogeneous porous media. Second, specific surface Brunauer–Emmett–Teller (BET) analysis was conducted and used for estimation of VOC isotherm parameters in soil. Finally, two models were fitted for VOC emission prediction, and the results were compared to the experimental emission results. It was found that free diffusion mode worked well, and an empirical correction factor seems to be needed for the other model to adapt to our condition for single and binary systems.

Keywords Crude oil · VOC · Evaporation · Environmental hydrocarbons · Sandy soil · Petroleum

Introduction

The prediction of crude oil volatile organic compound (VOC) evaporation and diffusion behavior is vital for remote emission detection and risk assessment of contaminated sites. Because typical crude oils could lose up to 45 % of their volume within a few days (Fingas 2013), most of which were VOCs. These fractions were demonstrated to have ecotoxicological effects on bacteria and significantly inhibited the ecological recolonization (Erlacher et al. 2013; Rico-Martinez et al. 2013). Therefore, studies were conducted to remove petroleum hydrocarbons with surfactant-induced remediation (Ghosh and Tick 2013; Torabian et al. 2010). However, in the burst of belowground crude oil pipeline spill pollution, it is vital to know the amount of crude oil VOCs sorbed to soil surfaces and how fast they will diffuse through the soil pores into the atmosphere, which are helpful for remote oil spill detection (Singha et al. 2013).

A determinative method with minimized matrix effects is needed for crude oil VOC quantification. Headspace solid-phase microextraction (HS-SPME) was developed for this purpose (Arthur and Pawliszyn 1990). Besides being simple, rapid, and inexpensive, HS-SPME is completely solvent-free and can be automated easily (Zhang and Pawliszyn 1993). For further application in a nonsteady-state mass transfer situation, a method for nonequilibrium extraction was proposed (Ai 1997, 1998) and popularly employed (Psillakis et al. 2012a;

Responsible editor: Michael Matthies

H. Wang (✉) · T. Fischer
Central Analytical Laboratory, Brandenburg University of
Technology Cottbus-Senftenberg, Konrad-Wachsmann-Allee 6,
03046 Cottbus, Germany
e-mail: whj2011@gmail.com

W. Wieprecht · D. Möller
Brandenburg University of Technology Cottbus-Senftenberg,
Volmerstr. 13, 12489 Berlin, Germany

Psillakis et al. 2012b). Different HS-SPME fibers were selected for crude oil hydrocarbon analysis (Baedecker et al. 2011; Ramsey et al. 2009; Tang and Isacson 2008; Van Hamme and Ward 2000). In our pre-study, a synergistic effect from crude oil VOCs took place on 100- μm polydimethylsiloxane (PDMS) SPME fiber, which should be taken into consideration for VOC mixture analysis.

Long-term sorption behaviors of crude oil VOCs, including the main rules and mechanisms of sorption were previously studied (Breus and Mishchenko 2006; Ran et al. 2005). The influence of VOC polarity on soil mineral sorption was shown to obtain a higher soil adsorption for polar compared to aliphatic and aromatic compounds (Ruiz et al. 1998). A prediction method for gas-phase VOC isotherms onto soils and soil constituents was developed (Campagnolo and Akgerman 1996). Prediction models for adsorption and desorption of VOCs revealed a competition with co-adsorbate during dynamic sorption (Guo et al. 1998; ThibaudErkey et al. 1996; Thoma et al. 1999).

Detection and simulation methods were frequently studied for oil spill monitoring and environmental risk assessments at crude oil-contaminated sites for oil spill in seawater and coastal area (Conmy et al. 2014; Hong et al. 2012; Zhang et al. 2013). Due to the pipeline cracking, underground oil spill is also an important and meaningful subject, which should be taken notice of. Reliable prediction of the unsaturated zone transport and attenuation of dissolved-phase VOC is an important problem, as the sources perhaps persist for decades including solid-waste landfills, aqueous-phase liquid discharge, and nonaqueous-phase liquid (NAPL) releases partially penetrating the unsaturated zone (Rivett et al. 2011). The development and application of analytical and semianalytical solutions were conducted as diffusive transport equations to predict emission rates from contaminated soils and sediments that have their moisture content changing with time (Choy et al. 2001). Subsequently, volatile organic total concentrations in the unsaturated zone could be estimated based on soil air analysis combined with determination of basic physico-chemical soil characteristics (Zdravkov et al. 2009). Soil surface modification was also used to reduce the spread of VOCs (Peng et al. 2012).

In this study, the goals of investigation were as follows: (1) to develop an applicable determinative method for a crude oil binary VOC (*n*-pentane and *n*-hexane) system with headspace SPME under nonequilibrium mass transfer conditions, which is suitable for infield sampling; (2) to obtain sorption isotherm parameters of these nonpolar VOCs in soil minerals using specific surface Brunauer–Emmett–Teller (BET) analysis to know the interaction between soil minerals and crude oil VOCs and to calculate the soil-air equilibrium partitioning coefficient; and (3) to predict binary VOC diffusion flux from sandy soil with the adapted model and to compare the predicted results with experimental flux value.

Theory

Nonequilibrium mass transfer analysis with SPME

Under nonequilibrium mass transfer state in headspace, a model (Eq. 1) was proposed for SPME to handle such conditions, which was later improved to work out better for real situations (Eq. 2) (Ai 1997, 1998).

$$n = n^\infty [1 - \exp(-a_{ht})] \quad (1)$$

$$n = \alpha [1 - \exp(-bt)] + \beta [1 - \exp(-dt)] \quad (2)$$

Liquid evaporation

A model was proposed for liquid evaporation over an area of a , which was described by Eqs. 3–5 (Stiver and Mackay 1984). We defined $kaPv/V_0RT$ in Eq. 3 as K_e , so that the evaporated volume fraction change with time t can be described as Eq. 6.

$$N = kaP/(RT) \quad (3)$$

$$dF_v/dt = kaPv/(V_0RT) \quad (4)$$

$$dF_v = [Pv/(RT)](ka dt/V_0) \quad (5)$$

$$F_v = K_e \cdot t \quad (6)$$

BET isotherm parameters estimation

Adsorption isotherms of various nonpolar VOCs were turned out to be similar on dry soils and clay minerals (Campagnolo and Akgerman 1996). Therefore, the BET isotherm parameters were empirically estimated (Eqs. 7–10).

$$\alpha_m = 1.091 \left(\frac{M}{N_0 \rho} \right)^{2/3} \quad (7)$$

$$S_m = \left(\frac{W_m N_0}{M} \right) \alpha_m \quad (8)$$

$$W_{m,voc} = \frac{0.70 M S_{m,N_2}}{\alpha_{m,voc} N_0} \quad (9)$$

$$W_{voc} = W_{N_2} \left(\frac{W_{m,voc}}{W_{m,N_2}} \right) \quad (10)$$

Model for diffusion flux through soil layer

To predict emission rates from contaminated soils and sediments that have their moisture content changing with time, diffusive transport equations were used (Choy et al. 2001). The applicative equation for our experiments was deduced as Eq. 11. BET isotherm parameters estimation was used for $K_{d,dry}$ calculation (Eq. 12). The model for $D_{A(eff)}$ approximation was presented in Eq. 13 (Millington and Quirk 1961).

$$J_A(t) = D_{A(eff)} C_{A0} \left\{ \frac{1}{L} + \frac{2L(\varepsilon + \rho_b K_d)}{\pi^2 D 2t} \exp \left[\left(\frac{\pi}{L} \right)^2 \frac{-D_{A(eff)} t}{\varepsilon + \rho_b K_d} \right] \right\} \quad (11)$$

$$K_{d,dry} = \frac{W_{mA}}{P_A^{sat}} \exp \left(\frac{\Delta H_{cond} - \Delta H_{ads}}{RT} \right) \quad (12)$$

$$D_{A(eff)} = D_A \frac{\varepsilon_{air}^{10/3}}{(\varepsilon_{air} + \varepsilon_{water})^2} \quad (13)$$

Materials and methods

Materials

n-Pentane (>99 % pure) and *n*-hexane (>99.9 % pure) were purchased from Baker Analyzed and Merck, respectively. The total organic carbon contents (TOC) of the used sandy soil were 0.41 %, and the porosity is 0.33. Before used, the soil was dried at 105 °C for 24 h. The sampling location was located near Lieberose, Brandenburg, northeast Germany (51° 55' 49" N, 14° 22' 22" E). All samples were used as received.

GC experiments and SPME conditions

GC conditions The chromatographic analysis was performed using a Hewlett Packard 5890 Series II gas chromatograph (GC) coupled with flame ionization detector (GC-FID), with a split-splitless injector operating in splitless mode for 0.5 min and a 60-m length, 0.32-mm I.D., 1.8-μm film thickness Rtx®-502.2 column. The injector and detector temperatures were 250 °C; the carrier gas was helium at 1 mL min⁻¹. The temperature program was as follows: 40 °C for 5 min, then ramped to 250 °C at a step of 5 °C min⁻¹ and held at 250 °C for 20 min. All samples (Table 1) were analyzed in duplicate or triplicate.

SPME The 100-μm PDMS SPME fiber with manual holder was purchased from Supelco Analytical. Conditioning at

Table 1 Retention times (*t*), correlation coefficient (*R*), linearity, relative standard deviation (*RSD*), and limits of detection and quantification (LOD, LOQ) of *n*-pentane and *n*-hexane

Compound	<i>t</i> (min)	<i>R</i>	Linearity (g m ⁻³)	RSD (%)	LOD (g m ⁻³)	LOQ (g m ⁻³)
<i>n</i> -Pentane	5.175	0.9979	0.062–112.727	2.74	<0.062	<0.062
<i>n</i> -Hexane	8.500	0.9981	0.066–120.000	2.74	<0.066	<0.066

250 °C for 0.5 h of the SPME fiber was performed according to the Guideline (T794123T Sigma-Aldrich: Solid-Phase Microextraction Fiber Assemblies). Absorption time of 2 min was conducted in the headspace of the sample, followed by 4-min desorption in the gas chromatography injection port. The sensitivity of GC was controlled with standards.

BET isotherm tests

Autosorb-AS1 from the company Quantachrome was employed for BET analysis with liquid nitrogen. Triplicate experiments were performed for sandy soil BET adsorption isotherm analysis. The soil used for BET isotherm tests was dried at 105 °C for 24 h with the bulk density of 1.622 kg L⁻¹ and sampled randomly for analysis.

Binary VOCs (*n*-pentane and *n*-hexane) diffusion experiments

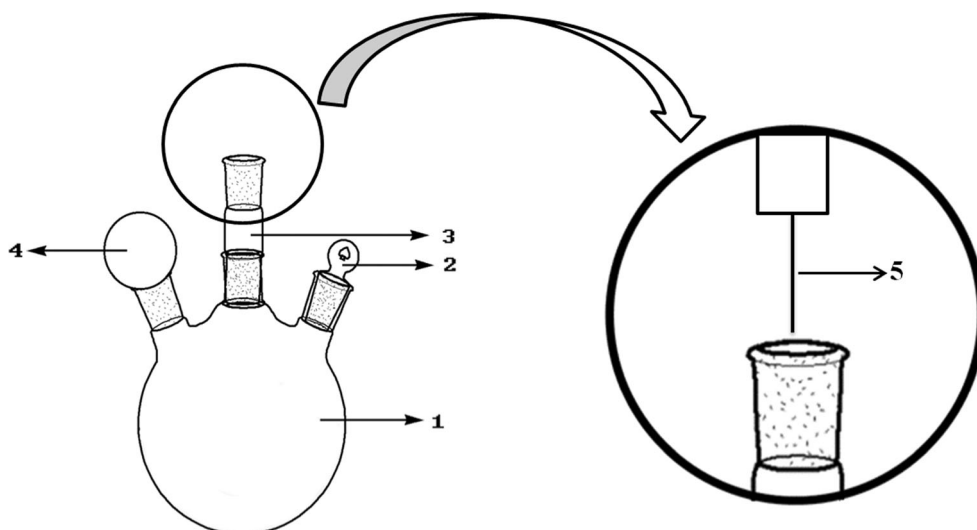
A 2.5 cm high and 2 cm in diameter glass column was filled with sandy soil to a height of 0.5 cm. The soil was dried at 105 °C for 24 h with the bulk density of 1.622 kg L⁻¹ and sampled randomly for diffusion experiments. The soil was based on the support of a glass cotton ball, which was proved to have little influence on VOC free diffusion during pre-experiments. One of the flask necks was sealed with a plug (Fig. 1). Another neck was connected with a balloon to control the inside pressure of the flask to be ambient pressure. Binary VOC system evaporation was studied in this 250-mL three-neck flask. All experiments were handled at a temperature of 24.5±0.5 °C.

Results

VOCs BET isotherm parameters

The isotherm predictive method for various nonpolar VOCs was proposed by Campagnolo and Akgerman (1996), which is applicable to crude oil VOCs. As shown in Fig. 2, the response 1/[*W*/(*P*₀/*P* - 1)] of nitrogen in experiments increased with relative pressure *P*/*P*₀ (0.05–0.31) in the sandy soil BET analysis, which was the arithmetic mean of three

Fig. 1 Schematic illustration for device used for binary VOC evaporative experiment. The numbers 1–5 stand for flask, plug, glass column, balloon, and SPME fiber, respectively



replicates. The specific sandy soil surface area averaged to $0.271 \text{ m}^2 \text{ g}^{-1}$.

In Fig. 2, slope and intercept of the isotherm curve are $(C_{BET} - 1)/(C_{BET} * W_m)$ and $1/(C_{BET} * W_m)$, respectively. BET constant C_{BET} and W_m (the amount adsorbed corresponding to monolayer surface coverage) of nitrogen can be deduced from isotherm parameters.

The projected area of a single adsorbate molecule α_m was computed by Eq. 7 for nitrogen and VOCs. Surface area covered by a unimolecular layer S_m for nitrogen was obtained by Eq. 8. Equations 9 and 10 were used for calculation of $W_{m,voc}$ (the mass of adsorbed monolayer molecules per unit weight soil) and W_{voc} (the mass adsorbed onto a unit weight soil). We assumed the C_{BET} value of nitrogen as that of our VOCs, due to unobvious impact on the shape of isotherm for VOCs in the range of 0–0.3 for P/P_0 (Campagnolo and Akgerman 1996).

VOC adsorption isotherms were predicted as shown in Fig. 2. As expected, $1/[W/(P_0/P - 1)]$ increased along with

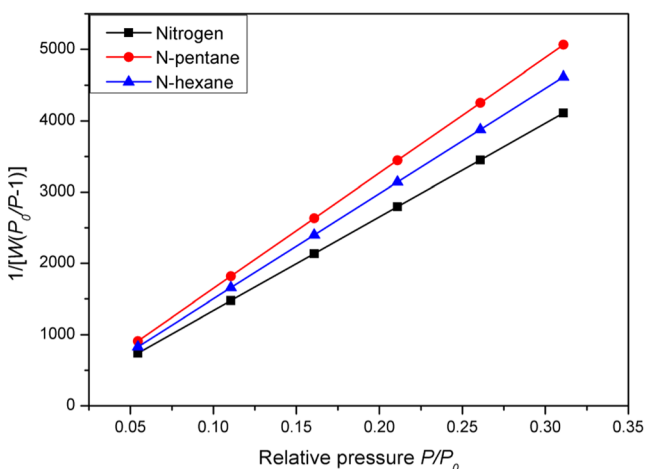


Fig. 2 BET analysis results for nitrogen isotherm and adsorption isotherm prediction for *n*-pentane and *n*-hexane on sandy soil

the relative pressure P/P_0 (0.05–0.31). When pure VOC was adsorbed to sandy soil, the adsorption amount $W_{n\text{-pentane}}$ and $W_{n\text{-hexane}}$ increased from 6.330×10^{-5} to 8.910×10^{-5} g per gram soil and from 6.947×10^{-5} to 9.777×10^{-5} g per gram soil, respectively. In condition of pure adsorption, the monolayer soil surface areas S_m covered by *n*-pentane and *n*-hexane were nearly the same, about $0.186 \text{ m}^2 \text{ g}^{-1}$. Calculation of K_d (soil-air equilibrium partition coefficient) at dry condition was done with the projected data above.

Calibration for binary VOCs system with SPME

To test for the influence from the synergistic effect of the VOCs mixture on 100- μm PDMS SPME fiber, the highest calibration concentration 112.727 g m^{-3} of *n*-pentane was analyzed both in pure condition and with *n*-hexane 1:1 (volume) as binary system. The relative standard deviation (RSD) for pure *n*-pentane and *n*-pentane in VOC mixture was 6.7 % (Fig. 3).

Analytical method validation

Table 1 summarizes the determination result for *n*-pentane and *n*-hexane. Calibration was validated with *n*-pentane and *n*-hexane as 1:1 mixture in a glass device. Precision and linearity were assessed by double or triple injection. The linearity range for *n*-pentane was from 0.062 to 112.727 g m^{-3} with a RSD less than 2.74 % on six levels, and the correlation coefficient (R) was 0.9979. The limit of detection (LOD) and limit of quantification (LOQ) for *n*-pentane were both below 0.062 g m^{-3} . *n*-Hexane was calibrated from 0.066 to 120.000 g m^{-3} with a R value of 0.9981 and RSD also less than 2.74 %. The LOD and LOQ for *n*-hexane were both below 0.066 g m^{-3} .

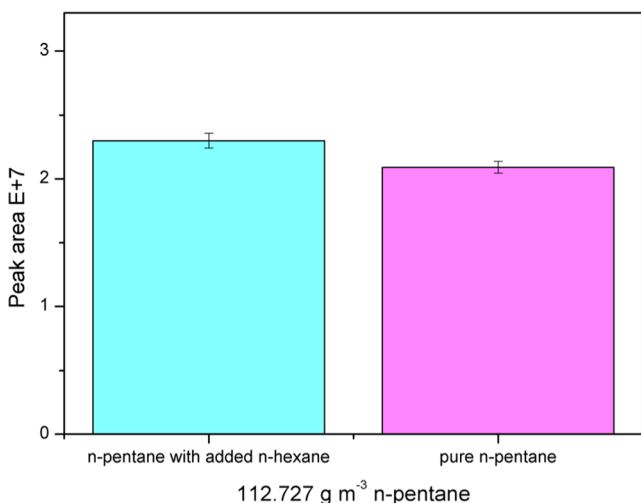


Fig. 3 n-Pentane GC signal fluctuation influenced by synergistic effect from hexane analyzed by 100- μm PDMS SPME fiber, at the highest calibration concentration of 112.727 g m^{-3} . The amount ratio of *n*-pentane and *n*-hexane is 1:1

VOCs evaporation into air by free diffusion

Binary VOC free diffusion was compared with pure *n*-pentane free diffusion (Fig. 4). Pure *n*-pentane (6.367 g) was put into the flask for previous free diffusion experiment. The free diffusion rate for pure *n*-pentane was rapid at an average velocity of $0.678\text{ g m}^{-2}\text{ s}^{-1}$ in the first 30 min and then slowed down to nearly constant evaporation rate about $0.349\text{ g m}^{-2}\text{ s}^{-1}$ in a long run (about 14 h). Artificial binary VOC mixture with 6.769 g *n*-pentane and 5.811 g *n*-hexane was injected into the flask for free diffusion study. In the first 30 min, a velocity of $0.409\text{ g m}^{-2}\text{ s}^{-1}$ was observed, and then averagely stabilized to $0.202\text{ g m}^{-2}\text{ s}^{-1}$. With Eqs. 3–6, theoretical prediction for binary VOCs was calculated with flask neck area and

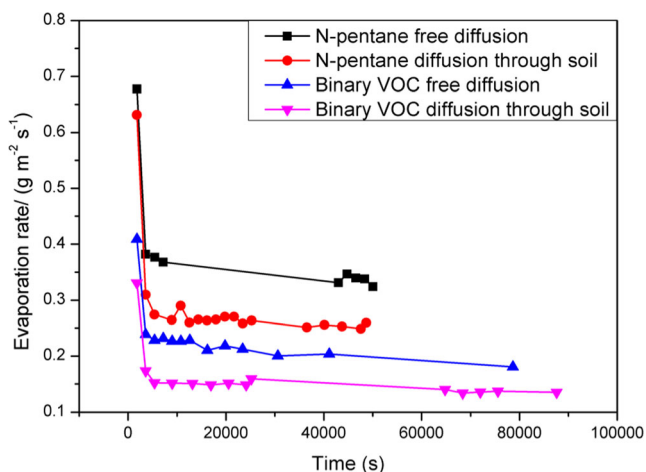


Fig. 4 Evaporation rate comparison of *n*-pentane free diffusion, *n*-pentane diffusion through soil, binary VOC (*n*-pentane and *n*-hexane) free diffusion, and binary VOC diffusion through soil

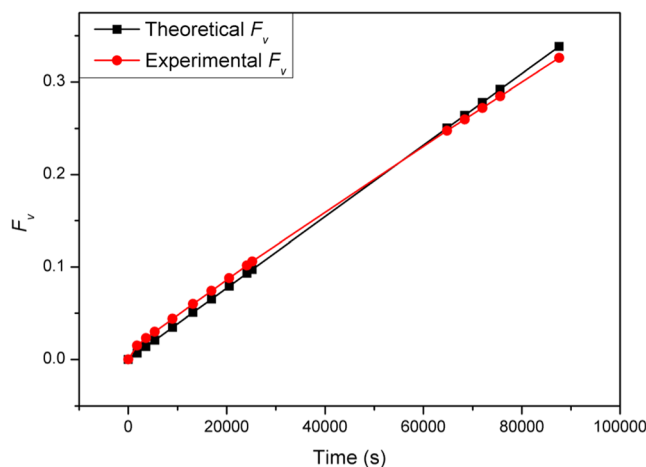


Fig. 5 Theoretical and experimental results for binary VOC free diffusion. *Y*-axis evaporated volume fraction F_v , changed with *X*-axis time

compared to experimental results (Fig. 5). Theoretical and experimental results correlated with $R=0.999$, $p<0.001$ (Pearson’s product-moment correlation, Fig. 5). *n*-Pentane and *n*-hexane saturated vapor pressures at $24.5\text{ }^\circ\text{C}$ were 67, 073 and 19,733 Pa, respectively. The binary VOC vapor pressure was 47,277 Pa, calculated according to Raoult’s law at $24.5\text{ }^\circ\text{C}$.

With the SPME method described above, binary evaporation concentration levels were distinctly determined. As shown in Fig. 6, both *n*-pentane and *n*-hexane showed a concentration gradient of 2-cm depth inside the flask to top of the flask neck. The experiments were repeated twice or in triple to ensure precision. According to Fick’s law, the free diffusion coefficient was estimated for VOCs, which can be used for the prediction of effective diffusion coefficient with Eq. 13.

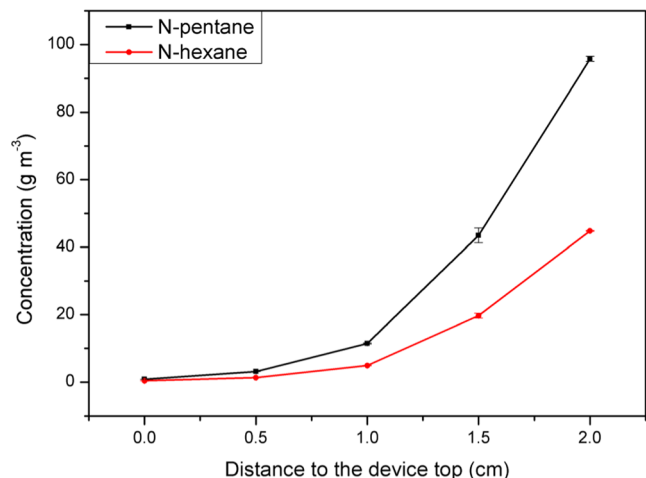


Fig. 6 *n*-Pentane and *n*-hexane concentration level in the device during free diffusion, due to the influence from gravity. Error bars represent standard error of mean ($n=2$ or 3)

VOCs evaporation through sandy soil layer

The diffusion flux decreased significantly both for pure *n*-pentane and binary VOC system, when sandy soil layer was put into the flask neck. In a long run, pure *n*-pentane approached to a constant value of approximately $0.275 \text{ g m}^{-2} \text{ s}^{-1}$ and binary VOCs system equilibrated to $0.146 \text{ g m}^{-2} \text{ s}^{-1}$, which was obviously distinct from free diffusion (Fig. 4). For binary VOCs at 0.5 cm above the soil surface, *n*-pentane concentration reduced from 3.178 to 1.842 g m^{-3} and *n*-hexane from 1.332 to 0.720 g m^{-3} , without and with soil, respectively.

With Eqs. 3–6, an evaporation prediction through sandy soil layer was done for binary VOCs (Fig. 7). Substantially evaporated volume fraction F_v coincided for the theoretical and experimental results ($R=0.999$, $p<0.001$, Pearson's product-moment correlation).

Binary VOC evaporation through sandy soil—model parameters

Parameters for Eq. 11 are listed in Table 2. K_d was the soil-air equilibrium partition coefficient, which was predicted using Eq. 12 with the data of BET analysis. ε is the porosity of soil medium, which is sand in our study and which was determined after complete water saturation using a pF apparatus. L is the characteristic length of soil layer, which was set to 0.005 m . C_{A0} is the mobile phase species A concentration under the soil layer, which was determined using SPME. ρ_b is the bulk density of soil, which was tested three times to obtain an average. $D_{A(\text{eff})}$ is effective diffusion coefficient of species A, calculated from Eq. 13. Finally, the J_A for binary VOCs is deduced as $0.187 \text{ g m}^{-2} \text{ s}^{-1}$, which is larger than experimental value $0.146 \text{ g m}^{-2} \text{ s}^{-1}$.

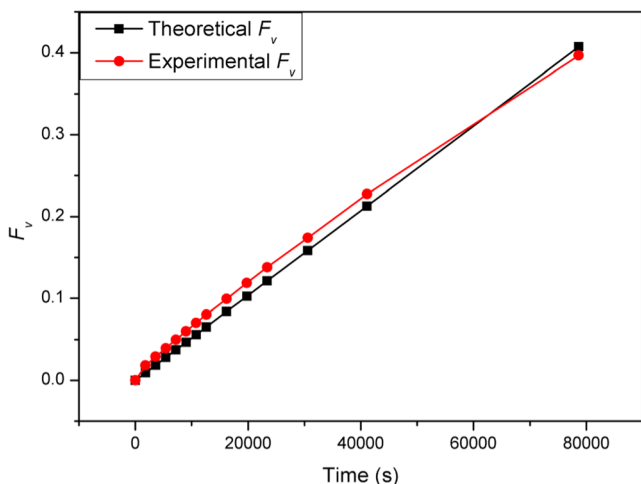


Fig. 7 Theoretical and experimental results for binary VOC diffusion through 0.5-cm soil layer. Y-axis evaporated volume fraction F_v changed with X-axis time

Table 2 Data summary for calculating *n*-pentane and *n*-hexane evaporation through soil flux with the predictive model

Parameters	<i>n</i> -Pentane	<i>n</i> -Hexane
K_d ($\text{kg kg}^{-1}/\text{kg m}^{-3}$)	1.572E-12	5.867E-12
ε	0.33	0.33
L (m)	0.005	0.005
C_{A0} (kg m^{-3})	0.043	0.020
ρ_b (kg m^{-3})	1622.363 ± 5.102	1622.363 ± 5.102
$D_{A(\text{eff})}$ ($\text{m}^2 \text{ s}^{-1}$)	1.49E-05	1.45E-05

Discussion

Binary VOCs determination with SPME

Since the nonequilibrium determination with SPME has come up with (Ai 1997, 1998), it was successfully used and verified by other researchers (Psillakis et al. 2012a; Psillakis et al. 2012b). Our study was carried out in a nonsteady-state mass transfer process with a $100\text{-}\mu\text{m}$ PDMS SPME fiber, and each calibration point was double or triply repeated to confirm precision. Our previous study presented a synergistic effect on this $100\text{-}\mu\text{m}$ PDMS SPME fiber, when crude oil VOCs mixture was extracted. At high concentration, $100 \mu\text{m}$ PDMS SPME fiber showed poor precision for VOC mixture and was unqualified for quantification. So, a shifting at the highest calibration concentration 112.727 g m^{-3} for *n*-pentane was tested to control the influence of the synergistic effect (Fig. 3). The RSD for pure *n*-pentane and *n*-pentane in mixture was 6.7% at 112.727 g m^{-3} , so the calibration method was applicable in our study.

VOCs free diffusion

The VOC evaporation behavior was influenced by the number of components contained in crude oil (Fingas 1997). Pure compounds evaporated in a linear manner, and multicomponent crude oil mixture evaporated in a logarithmic manner (Okamoto et al. 2012). Previous studies showed that crude oil evaporation was empirically represented depending only on time and temperature (Fingas 2013).

Our preceding study on pure *n*-pentane showed evaporated volume fraction and time accorded in a linear manner. Binary VOC evaporation studied in this paper showed the same linear behavior (Fig. 5). The vapor pressure might have significant influence on VOC evaporation velocity. This agreed with the empirical consequence for crude oil evaporation (Fingas 2004), which showed that crude oil evaporated percentage was only related with temperature, besides time. Because the temperature was the only factor, that influences the vapor pressure (Antoine equation). When less volatile VOCs are further added to the evaporation system, the vapor pressure

decrease would be supposed to become more significant, leading to even lower evaporation velocity.

Equation 6 is a deduced equation from previous research (Stiver and Mackay 1984). In our study, the semienclosed flask volume influenced the evaporation at first and the flask neck area a started to control the evaporation process until flask vapor saturation. The parameter K_e is $kaPv/V_0RT$ in Eq. 6. The group a/V_0RT is constant, and kPv is somehow shifting as evaporation proceeded in our specialized system, which is the reason that the theoretical and experimental F_v differed slightly (Figs. 5 and 7). However, the volume and crude oil content can be assumed to be infinite and invariable during the short evaporation period in crude oil spill, where the kPv variation influence might be minimal. The high density of the binary VOC gas mixture was probable to result in concentration gradient in the flask.

VOCs evaporation prediction through sandy soil with free diffusion model

A hydrocarbon surface evaporation model (Stiver and Mackay 1984) was used for prediction of crude oil binary VOC system evaporation through the sandy soil layer (Eqs. 3–6). Since a/V_0RT is constant and kPv is shifting not much for free diffusion, parameter K_e was assumed to be a constant value.

To do calculation for mass transfer coefficient k , experiments for short-period evaporation were needed to obtain evaporation rates with Eq. 3. The group kPv was assumed to keep a constant value as evaporation started. With known a/V_0RT , K_e was obtained to predict the evaporation process. In Fig. 7, theoretical and experimental evaporated volume fraction was compared. The shifting reason seemed similar to binary VOC free diffusion. The free diffusion model was used to predict the percentage evaporated within a random period of time, which approximately conformed to the actual situation.

Experimental and predictive evaporation flux analysis and comparison

With the sandy soil layer, the volume of the flask controlled the evaporation in the first 30 min. Then, the evaporation rate turned to be a constant lower value than free diffusion in a short time (Fig. 4). Under conditions of pure adsorption, the monolayer soil surface areas S_m covered by n -pentane and n -hexane were nearly the same and amounted to approximately $0.186 \text{ m}^2 \text{ g}^{-1}$, which would average as $0.186 \text{ m}^2 \text{ g}^{-1}$ for the mixture. The total surface area averaged to $0.271 \text{ m}^2 \text{ g}^{-1}$, of which $0.186 \text{ m}^2 \text{ g}^{-1}$ was occupied by VOCs from evaporation. The TOC content of the used sandy soil was 0.41 %, which indicates that the VOCs underwent mainly physical adsorption. Therefore, with little chemical sorption and evaporation passage, VOC saturation would be completed soon.

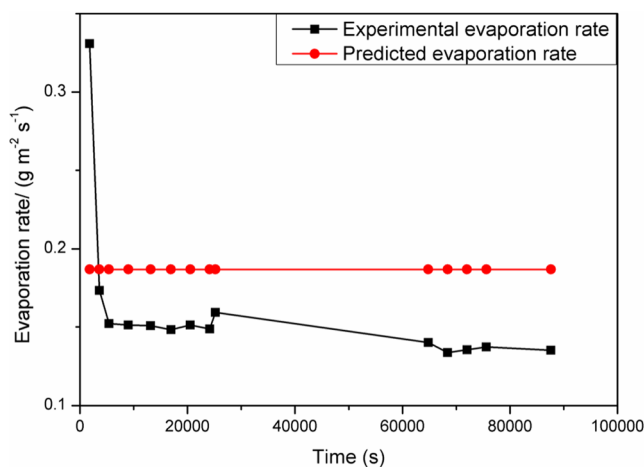


Fig. 8 Experimental and predictive results for binary VOC diffusion through soil. Experimental value was 78.15 % of the model predicted diffusion flux value averagely

For binary VOCs, experimental evaporation flux was $0.146 \text{ g m}^{-2} \text{ s}^{-1}$, which was about 78 % of the predictive value $0.187 \text{ g m}^{-2} \text{ s}^{-1}$ (Fig. 8) with Eq. 11. In our previous study, pure n -pentane had an experimental flux value of $0.275 \text{ g m}^{-2} \text{ s}^{-1}$, 74 % of the model deducing value $0.370 \text{ g m}^{-2} \text{ s}^{-1}$. Two reasons probably influenced the difference between the theoretical and experimental values. One was the n -pentane vapor density, which might result in concentration on different air levels (Fig. 6) and C_{A0} in Eq. 11 would gain some deviation due to this reason. The other reason is the model was originally developed for the condition (Choy et al. 2001) that the concentration at the top of the soil surface is zero, neglecting the mass transfer resistance in the air. However, in our study of the binary VOC system at 0.5 cm above the soil surface, n -pentane concentration was 1.842 g m^{-3} and n -hexane was 0.720 g m^{-3} . For single and binary VOC systems, it seems that an empirical correction factor around 0.74–0.78 is needed for the prediction model (Eq. 11) to adapt to our experimental situation.

Conclusion

A determination headspace-SPME-GC method was established for crude oil binary VOCs in a nonsteady-state mass transfer process, with acceptable synergistic effect on 100- μm PDMS SPME fiber. With BET analysis for nitrogen, VOC absorption amount to the sandy soil and monolayer soil surface area covered by VOCs were deduced, which revealed that 68.6 % of the soil surface was occupied by studied VOCs under mainly physical adsorption. Two modes were tried to predict VOC diffusion through the sandy soil layers. Free diffusion mode worked well with available experimental data for VOCs evaporation. An empirical correction factor seems to be needed for the other model to adapt to our condition for

single and binary VOC evaporation systems. Further study for more complex VOC matrix will proceed.

Notation

n	The amount of analyte extracted by the SPME before partition equilibrium (mol)
n^∞	The amount of analyte extracted by the SPME at partition equilibrium (mol)
a_h	A empirical parameter determines how fast the equilibrium can be reached
α	Integration constant
β	Integration constant
b	Empirical parameter determined in an experimental system
d	Empirical parameter determined in an experimental system
N	Molar flux (mol s^{-1})
k	Mass transfer coefficient (m s^{-1})
a	Oil spill area (m^2)
P	Liquid vapor pressure (Pa)
P_0	Adsorbate saturation pressure (Pa)
R	Gas constant ($8.314 \text{ Pa m}^3 \text{ mol}^{-1} \text{ K}^{-1}$)
T	Environmental temperature (K)
F_v	Volume fraction evaporated
K_e	Evaporated volume fraction coefficient (s^{-1})
t	Time (s)
v	Liquid's molar volume ($\text{m}^3 \text{ mol}^{-1}$)
V_0	Initial volume of spilled liquid (m^3)
α_m	Projected area of a single adsorbate molecule (nm^2)
M	The molecular weight of the adsorbate (g mol^{-1})
N_0	Avagadro's number (6.022×10^{23})
ρ	Density (kg m^{-3})
S_m	Surface area covered by a unimolecular layer (m^2)
W_m	Mass of an adsorbed monolayer of molecules per unit weight of soil ($\text{kg kg}^{-1} \text{ soil}$)
W	Mass adsorbed onto a unit weight of soil ($\text{kg kg}^{-1} \text{ soil}$)
J_A	Mass flux of component A ($\text{kg m}^{-2} \text{ s}^{-1}$)
$D_{A(\text{eff})}$	Effective diffusion coefficient of species A ($\text{m}^2 \text{ s}^{-1}$)
C_A	Mobile phase species A concentration (kg m^{-3})
L	Characteristic length of soil layer (m)
ε	Porosity of the medium
ρ_b	Bulk density of the porous medium (kg m^{-3})
K_d	Soil-air equilibrium partition coefficient ($\text{kg kg}^{-1} \text{ (soil)}/\text{kg m}^{-3} \text{ (air)}$)
π	3.14

Acknowledgments The authors are grateful to Regina Mueller and Gabriele Franke for helping the BET analysis. The authors would like to thank the Arbeitsgemeinschaft Industrieller Forschungseinrichtungen, the Gesellschaft zur Förderung der atmosphärischen Umweltforschung

GEFU e.V., and the Institut für nachhaltigen Umweltschutz INU GbR for financial support, as well as Philipp Lange for technical assistance.

References

- Ai J (1997) Headspace solid phase microextraction. Dynamics and quantitative analysis before reaching a partition equilibrium. *Anal Chem* 69:3260–3266
- Ai J (1998) Solid phase microextraction in headspace analysis. Dynamics in non-steady state mass transfer. *Anal Chem* 70:4822–4826
- Arthur CL, Pawliszyn J (1990) Solid phase microextraction with thermal desorption using fused silica optical fibers. *Anal Chem* 62:2145–2148
- Baedecker MJ, Eganhouse RP, Bekins BA, Delin GN (2011) Loss of volatile hydrocarbons from an LNAPL oil source. *J Contam Hydrol* 126:140–152
- Breus IP, Mishchenko AA (2006) Sorption of volatile organic contaminants by soils (a review). *Eurasian Soil Sci* 39:1271–1283
- Campagnolo JF, Akgerman A (1996) A prediction method for gas-phase VOC isotherms onto soils and soil constituents. *J Hazard Mater* 49: 231–245
- Choy B, Reible DD, Valsaraj KT (2001) Volatile emissions from variable moisture content sediments. *Environ Eng Sci* 18:279–289
- Conny RN, Coble PG, Farr J, Wood AM, Lee K, Pegau WS, Walsh ID, Koch CR, Abercrombie MI, Miles MS, Lewis MR, Ryan SA, Robinson BJ, King TL, Kelble CR, Lacoste J (2014) Submersible optical sensors exposed to chemically dispersed crude oil: wave tank simulations for improved oil spill monitoring. *Environ Sci Technol* 48:1803–1810
- Erlacher E, Loibner AP, Kendler R, Scherr KE (2013) Distillation fraction-specific ecotoxicological evaluation of a paraffin-rich crude oil. *Environ Pollut* 174:236–243
- Fingas MF (1997) Studies on the evaporation of crude oil and petroleum products: I. the relationship between evaporation rate and time. *J Hazard Mater* 56:227–236
- Fingas MF (2004) Modeling evaporation using models that are not boundary-layer regulated. *J Hazard Mater* 107:27–36
- Fingas MF (2013) Modeling oil and petroleum evaporation. *J Pet Sci Res* 2
- Ghosh J, Tick GR (2013) A pore scale investigation of crude oil distribution and removal from homogeneous porous media during surfactant-induced remediation. *J Contam Hydrol* 155:20–30
- Guo Y, Thibaud-Erkey C, Akgerman A (1998) Gas-phase adsorption and desorption of single-component and binary mixtures of volatile organic contaminants on soil. *Environ Eng Sci* 15:203–213
- Hong S, Khim JS, Ryu J, Park J, Song SJ, Kwon BO, Choi K, Ji K, Seo J, Lee S, Park J, Lee W, Choi Y, Lee KT, Kim CK, Shim WJ, Naile JE, Giesy JP (2012) Two years after the Hebei spirit oil spill: residual crude-derived hydrocarbons and potential AhR-mediated activities in coastal sediments. *Environ Sci Technol* 46:1406–1414
- Millington R, Quirk JP (1961) Permeability of porous solids. *Trans Faraday Soc* 57:1200–1207
- Okamoto K, Hiramatsu M, Miyamoto H, Hino T, Honma M, Watanabe N, Hagimoto Y, Miwa K, Ohtani H (2012) Evaporation and diffusion behavior of fuel mixtures of gasoline and kerosene. *Fire Saf J* 49:47–61
- Peng YH, Chou SM, Shih YH (2012) Sorption interactions of volatile organic compounds with organoclay under different humidities by using linear solvation energy relationships. *Adsorption* 18:329–336
- Psillakis E, Mousouraki A, Yiantzi E, Kalogerakis N (2012a) Effect of Henry's law constant and operating parameters on vacuum-assisted headspace solid phase microextraction. *J Chromatogr A* 1244:55–60
- Psillakis E, Yiantzi E, Sanchez-Prado L, Kalogerakis N (2012b) Vacuum-assisted headspace solid phase microextraction: improved extraction of semivolatiles by non-equilibrium headspace sampling under reduced pressure conditions. *Anal Chim Acta* 742:30–36

- Ramsey SA, Mustacich RV, Smith PA, Hook GL, Eckenrode BA (2009) Directly heated high surface area solid phase microextraction sampler for rapid field forensic analyses. *Anal Chem* 81:8724–8733
- Ran Y, Xing BS, Rao PSC, Sheng GY, Fu JM (2005) Sorption kinetics of organic contaminants by sandy aquifer and its kerogen isolate. *Environ Sci Technol* 39:1649–1657
- Rico-Martinez R, Snell TW, Shearer TL (2013) Synergistic toxicity of Macondo crude oil and dispersant Corexit 9500A (R) to the *Brachionus plicatilis* species complex (Rotifera). *Environ Pollut* 173:5–10
- Rivett MO, Wealthall GP, Dearden RA, McAlary TA (2011) Review of unsaturated-zone transport and attenuation of volatile organic compound (VOC) plumes leached from shallow source zones. *J Contam Hydrol* 123:130–156
- Ruiz J, Bilbao R, Murillo MB (1998) Adsorption of different VOC onto soil minerals from gas phase: influence of mineral, type of VOC, and air humidity. *Environ Sci Technol* 32:1079–1084
- Singha S, Vespe M, Trieschmann O (2013) Automatic synthetic aperture radar based oil spill detection and performance estimation via a semi-automatic operational service benchmark. *Mar Pollut Bull* 73:199–209
- Stiver W, Mackay D (1984) Evaporation rate of spills of hydrocarbons and petroleum mixtures. *Environ Sci Technol* 18:834–840
- Tang B, Isacson U (2008) Analysis of mono- and polycyclic aromatic hydrocarbons using solid-phase microextraction: State-of-the-art. *Energ Fuel* 22:1425–1438
- ThibaudErkey C, Guo Y, Erkey C, Akgerman A (1996) Mathematical modeling of adsorption and desorption of volatile contaminants from soil: Influence of isotherm shape on adsorption and desorption profiles. *Environ Sci Technol* 30:2127–2134
- Thoma G, Swofford J, Popov V, Soerens T (1999) Effect of dynamic competitive sorption on the transport of volatile organic chemicals through dry porous media. *Water Resour Res* 35:1347–1359
- Torabian A, Kazemian H, Seifi L, Bidhendi GN, Azimi AA, Ghadiri SK (2010) Removal of petroleum aromatic hydrocarbons by surfactant-modified natural zeolite: the effect of surfactant. *Clean-Soil Air Water* 38:77–83
- Van Hamme JD, Ward OP (2000) Development of a method for the application of solid-phase microextraction to monitor biodegradation of volatile hydrocarbons during bacterial growth on crude oil. *J Ind Microbiol Biot* 25:155–162
- Zdravkov B, Cermak JJ, Kucerova V, Kubal M, Janku J (2009) Gas survey techniques in soil environmental analysis. Interpretation, quantification and perspectives. Review. *J Environ Prot Ecol* 10: 944–953
- Zhang ZY, Pawliszyn J (1993) Analysis of organic compounds in environmental samples by headspace solid phase microextraction. *Hrc-J High Res Chrom* 16:689–692
- Zhang DY, Ding AZ, Cui SC, Hu C, Thornton SF, Dou JF, Sun YJ, Huang WE (2013) Whole cell bioreporter application for rapid detection and evaluation of crude oil spill in seawater caused by Dalian oil tank explosion. *Water Res* 47:1191–1200